International Journal of Non-Linear Mechanics 45 (2010) 100–110

Contents lists available at ScienceDirect

International Journal of Non-Linear Mechanics

journal homepage: www.elsevier.com/locate/nlm

Non-linear stability analysis of imperfect thin-walled composite beams

Sebastián P. Machado [a,b,*]

[a] Grupo Análisis de Sistemas Mecánicos, Facultad Regional Bahía Blanca, Universidad Tecnológica Nacional, 11de abril 461, B8000LMI Bahía Blanca, Argentina
[b] CONICET, Consejo Nacional de Investigaciones Científicas y Técnicas, Argentina

ARTICLE INFO

Article history:
Received 11 February 2009
Received in revised form
15 September 2009
Accepted 21 September 2009

Keywords:
Imperfection
Postbuckling
Non-linear behavior
Shear deformable beam theory
Ritz method

ABSTRACT

The static non-linear behavior of thin-walled composite beams is analyzed considering the effect of initial imperfections. A simple approach is used for determining the influence of imperfection on the buckling, prebuckling and postbuckling behavior of thin-walled composite beams. The fundamental and secondary equilibrium paths of perfect and imperfect systems corresponding to a major imperfection are analyzed for the case where the perfect system has a stable symmetric bifurcation point. A geometrically non-linear theory is formulated in the context of large displacements and rotations, through the adoption of a shear deformable displacement field. An initial displacement, either in vertical or horizontal plane, is considered in presence of initial geometric imperfection. Ritz's method is applied in order to discretize the non-linear differential system and the resultant algebraic equations are solved by means of an incremental Newton–Rapshon method. The numerical results are presented for a simply supported beam subjected to axial or lateral load. It is shown in the examples that a major imperfection reduces the load-carrying capacity of thin-walled beams. The influence of this effect is analyzed for different fiber orientation angle of a symmetric balanced lamination. In addition, the postbuckling response obtained with the present beam model is compared with the results obtained with a shell finite element model (Abaqus).

1. Introduction

This paper presents a theory to account for changes in the stability behavior of thin-walled composite beams when design parameters are modified. In particular, the model takes into account the influence of small deviations from the design configuration that occurs in the presence of imperfections. Determining this imperfection sensitivity is an important issue because imperfections in structures are inevitable and may result in very significant variations in the stability response. The buckling behavior of thin-walled beams is a difficult topic, since it involves the coupling among bending, twisting and stretching deformations of the beam member. For example, in the case of a beam subjected to a lateral load, the structure may fail in a flexural or/and torsional buckling mode: the beam suddenly deflects laterally or twists out of the plane of loading. In this case a non-linear theory is required for the accurate behavior prediction of such structures. The limitation of the linear buckling analysis of beam problems (e.g. Vlasov [1]) is the omission of any consideration of the prebuckling effect. This omission may be sufficiently accurate when the initial deflection, corresponding to the fundamental state, is negligible. In other cases, however, the effect of the prebuckling deflections must be taken into account for obtaining accurate predictions of buckling loads. In particular, lateral buckling is a relevant phenomenon [2] which involves mechanical complications, since structures may experience large or moderately large deflections and rotations before buckling occurs. The buckling and postbuckling analysis of thin-walled beams has been the subject of considerable research. However, most of these have been confined to metallic structures [3–14, for example]. Among the first works carried out for thin-walled beams, Barsoum and Gallagher [3] studied the torsional and flexural–torsional instability of a bisymmetric I-beam subjected to conservative loads. Woolcock and Trahair [4] carried out theoretical as experimentally studies on the postcritical behavior of thin-walled I-beams for different boundary conditions. A consistent co-rotational total Lagrangian formulation was presented by Hsiao and Lin [6–8] in the non-linear geometric analysis of mono- and bi-symmetric beams. In their formulation they considered third-order terms of the nodal forces, corresponding to the torsional twist. Based on Galerkin's method, Mohri et al. [9] studied the flexural–torsional and lateral postbuckling behavior of mono- and bi-symmetric simply supported beams, considering different load conditions. Pi and Bradford [10] used an accurate rotation matrix

* Correspondence address: Grupo Análisis de Sistemas Mecánicos, Facultad Regional Bahía Blanca, Universidad Tecnológica Nacional, 11de abril 461, B8000LMI Bahía Blanca, Argentina. Tel.: +54 0291 4555220; fax: +54 0291 4555311.
E-mail address: smachado@frbb.utn.edu.ar

0020-7462/$ - see front matter © 2009 Elsevier Ltd. All rights reserved.
doi:10.1016/j.ijnonlinmec.2009.09.006

in the formulation of a finite element model for the buckling and postbuckling analysis of thin-walled straight beams. Then, Pi and Bradford [11,12] and Pi et al. [13] extended their model to analyze the flexural–torsional stability response of arches with open thin-walled section under different radial loads. Recently, Machado [14] investigated the buckling and postbuckling behavior of simply supported, cantilever and fixed-end beams subjected to distributed or concentrated loads. He showed that the load-carrying capacity of elastic steel beams can be established only by using a non-linear buckling analysis.

On the other hand, laminated composites beams are increasingly being used in the design of load-carrying members especially in high-performance mechanical, aerospace, aircraft, naval and civil applications due to their outstanding engineering properties, such as high strength/stiffness to weight ratios. The interesting possibilities provided by fiber reinforced composite materials can be used to enhance the response characteristics of such structures that operate in complex environmental conditions. The new generation of these constructions should be designed to work in a safe way and to experience higher performance than the conventional systems. For example, composite laminates can often sustain large elongations up to the first occurrence of localized damage, in most instances the failure of thin-walled composite shapes is due to elastic buckling and the load carrying capacity is directly related to the critical buckling load. For this reason, knowledge of the postbuckling response and the ultimate load of such structures are essential for designers. In particular, this knowledge will allow composites to be designed efficiently and economically by fully exploiting their postbuckling strength. Bhaskar and Librescu [15] presented a geometrically non-linear theory for thin-walled composite beams, but postbuckling analyzes were not performed. The non-linear stability analysis of thin-walled composite beams with open section has been recently investigated by Fraternali and Feo [16], using a finite element formulation based on a second-order theory and disregarding shear-deformation. However, shear deformation effect plays an important role in the behavior of linear (Sapkás and Kollár [17], Machado and Cortínez [18], Morey et al. [19], Back and Will [20]) and non-linear (Machado and Cortínez [21]) stability of thin-walled composite beams, owing to the high ratio between the equivalent elasticity modulus and transverse elasticity modulus. Finally, Machado and Cortínez [21] investigated the flexural, torsional and flexural–torsional stability of simply supported beam subjected to axial and lateral load.

Sensitivity of postcritical states of imperfections (specifically geometric or load imperfections) has been the subject of research for some time and is part of the general theory of elastic stability (Thompson and Hunt [22]; Flores and Godoy [23]; Godoy [24]). Recently, Szymczak [25] and Chróscielewski et al. [26] investigated the dynamics and torsional buckling of a thin-walled bisymmetric simply supported beam, respectively. Szymczak [25] analyzed the relative variation of the first three eigenvalues due to the difference in the beam flanges. The influence of initial deflection on the torsional buckling load was investigated by Chróscielewski et al. [26]. They considered a thin-walled steel I-beam column axially loaded by two compressive forces. Most of the recent studies have been conducted toward the prediction of buckling and postbuckling behaviors of imperfect cylindrical laminated shell.

The objective of this publication is to analyze the influence of imperfections on the elastic stability of thin-walled composite beams. The fundamental and secondary equilibrium paths of perfect and imperfect systems corresponding to a major imperfection are analyzed for the case where the perfect system has a stable symmetric bifurcation point. To further clarify the problem studied, let us consider the response shown in Fig. 1. The horizontal axis represents the component of displacements and the vertical axis represents the load. It can be seen from Fig. 1 that the critical point disappears due to a major imperfection, where solid curves are the fundamental and equilibrium path of the original perfect structure, and the dashed lines correspond to the paths of the modified imperfect structures A geometrically non-linear theory is formulated to analyze this problem. The model is based on the context of large displacements and rotations, through the adoption of a shear deformable displacement field. An initial displacement, either in vertical or horizontal plane, is considered in presence of geometrical imperfections. Ritz's method is applied in order to discretize the non-linear differential system and the resultant algebraic equations are solved by means of an incremental Newton–Rapshon method. The numerical results are presented for a simply supported beam subjected to axial or lateral load. The influence of imperfections is analyzed for different fiber orientation angle of a symmetric balanced lamination. In addition, the numerical results obtained with the present beam theory are compared with those obtained from non-linear 6-parameter theory of a shell finite element model (Abaqus).

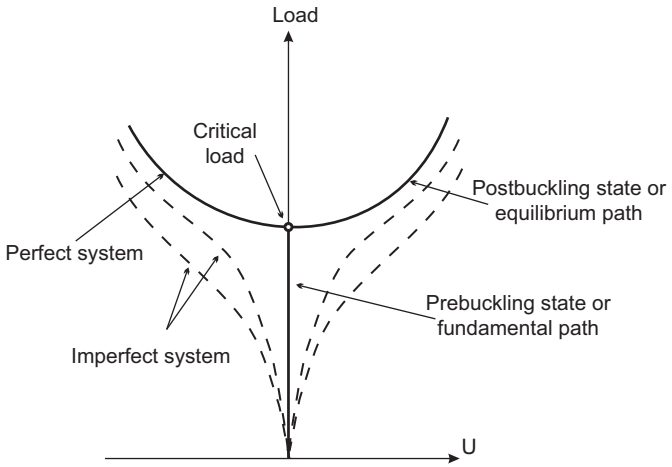

Fig. 1. Fundamental and secondary equilibrium paths of perfect and imperfect systems.

2. Kinematics

A straight thin-walled composite beam with an arbitrary cross-section is considered (Fig. 2). The points of the structural member are referred to a Cartesian coordinate system $(x,\overline{y},\overline{z})$, where the x-axis is parallel to the longitudinal axis of the beam while $\overline{y}$ and $\overline{z}$ are the principal axes of the cross-section. The axes y and z are parallel to the principal ones but having their origin at the shear center (SC), defined according to Vlasov's theory of isotropic beams. Midway through the thickness of each cross-sectional element is the middle surface. A plane perpendicular to the x-axis intersects the middle surface at a curve called the contour. The coordinates corresponding to points lying on the middle line are denoted as Y and Z (or $\overline{Y}$ and $\overline{Z}$). A contour (n, s, x) coordinate system is defined with s following the contour, and n perpendicular to s. This coordinate is introduced on the middle contour of the cross-section system.

$$\overline{y}(s,n)=\overline{Y}(s)-n\frac{dZ}{ds},\overline{z}(s,n)=\overline{Z}(s)+n\frac{dY}{ds}, \tag{1}$$

$$y(s,n)=Y(s)-n\frac{dZ}{ds},z(s,n)=Z(s)+n\frac{dY}{ds}. \tag{2}$$

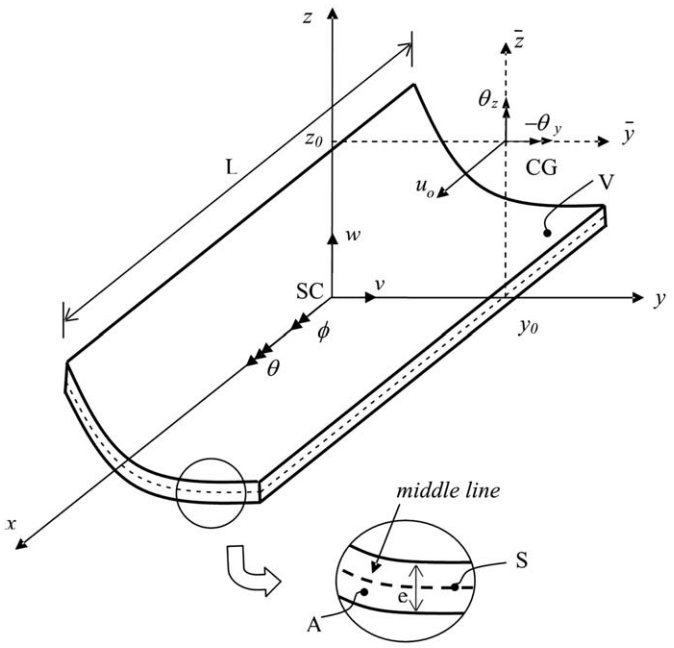

Fig. 2. General thin-walled section beam and notation for displacement measures.

On the other hand, y_0 and z_0 are the centroidal coordinates measured with respect to the shear center.

$$\overline{y}(s,n) = y(s,n) - y_0,$$

$$\overline{z}(s,n) = z(s,n) - z_0. \tag{3}$$

The present structural model is based on the following assumptions:

1. The cross-section contour is rigid in its own plane.
2. The warping distribution is assumed to be given by the Saint-Venant function for isotropic beams.
3. Flexural rotations (about the $\overline{y}$ and $\overline{z}$ axes) are assumed to be moderate, while the twist ϕ of the cross-section can be arbitrarily large.
4. Shell force and moment resultant corresponding to the circumferential stress σ_{ss} and the force resultant corresponding to the shear strain in the $n-s$ plane (γ_{ns}) are neglected.
5. The radius of curvature at any point of the shell is neglected.
6. Twisting linear curvature of the shell is expressed according to the classical plate theory.
7. The laminate stacking sequence is assumed to be symmetric and balanced, or especially orthotropic [27].

2.1. Development of the displacement field

According to the hypotheses of the present structural model, the displacement field proposed Eq. (4) is based on the principle of semitangential rotation defined by Argyris [21] to avoid the difficulty due to the non-commutative nature of rotations. In this displacement field, the torsional twist terms ϕ are expressed as trigonometric functions according to hypotheses (3). The displacement field is represented by means of seven degrees of freedom corresponding to three displacements (u, v and w), three measures of the rotations (ϕ, θ_y and θ_z) about the shear center axis, $\overline{y}$ and $\overline{z}$ axes, respectively; and a warping variable (θ) of the cross-section. The displacement field is expressed in the following form:

$$\begin{aligned}
u_x &= u_o - \overline{y}(\theta_z\cos\phi + \theta_y\sin\phi) \\
&\quad - \overline{z}(\theta_y\cos\phi - \theta_z\sin\phi) + \omega[\theta - \tfrac{1}{2}(\theta_y'\,\theta_z - \theta_y\theta_z')] + (\theta_z z_0 \\
&\quad - \theta_y y_0)\sin\phi, \\
u_y &= v - z\sin\phi - y(1-\cos\phi) - \tfrac{1}{2}(\theta_z^2\overline{y} + \theta_z\theta_y\overline{z}), \\
u_z &= w + y\sin\phi - z(1-\cos\phi) - \tfrac{1}{2}(\theta_y^2\overline{z} + \theta_z\theta_y\overline{y}),
\end{aligned} \tag{4}$$

where the prime indicates differentiation with respect to x. The warping function ω of the thin-walled cross-section is defined in [14]. The displacement field expression is a generalization of others previously proposed in the literature as is explained by the author in [14,21].

3. The strain field

The displacements with respect to the curvilinear system (x, s, n) are obtained by means of the following expressions:

$$\overline{U} = u_x(x,s,n), \tag{5}$$

$$\overline{V} = u_y(x,s,n)\frac{dY}{ds} + u_z(x,s,n)\frac{dZ}{ds}, \tag{6}$$

$$\overline{W} = -u_y(x,s,n)\frac{dZ}{ds} + u_z(x,s,n)\frac{dY}{ds}. \tag{7}$$

The three non-zero components ε_{xx}, ε_{xs}, ε_{xn} of the Green's strain tensor are given by:

$$\varepsilon_{xx} = \frac{\partial\overline{U}}{\partial x} + \frac{1}{2}\left[\left(\frac{\partial\overline{U}}{\partial x}\right)^2 + \left(\frac{\partial\overline{V}}{\partial x}\right)^2 + \left(\frac{\partial\overline{W}}{\partial x}\right)^2\right], \tag{8}$$

$$\varepsilon_{xs} = \frac{1}{2}\left[\frac{\partial\overline{U}}{\partial s} + \frac{\partial\overline{V}}{\partial x} + \frac{\partial\overline{U}}{\partial x}\frac{\partial\overline{U}}{\partial s} + \frac{\partial\overline{V}}{\partial x}\frac{\partial\overline{V}}{\partial s} + \frac{\partial\overline{W}}{\partial x}\frac{\partial\overline{W}}{\partial s}\right], \tag{9}$$

$$\varepsilon_{xn} = \frac{1}{2}\left[\frac{\partial\overline{U}}{\partial n} + \frac{\partial\overline{W}}{\partial x} + \frac{\partial\overline{U}}{\partial x}\frac{\partial\overline{U}}{\partial n} + \frac{\partial\overline{V}}{\partial x}\frac{\partial\overline{V}}{\partial n} + \frac{\partial\overline{W}}{\partial x}\frac{\partial\overline{W}}{\partial n}\right]. \tag{10}$$

Substituting expressions (4) into (5)–(7) and then into (8)–(10), after simplifying some higher order terms, the components of the strain tensor are expressed in the following form:

$$\begin{aligned}
\varepsilon_{xx} &= \varepsilon_{xx}^{(0)} + n\kappa_{xx}^{(0)}, \\
\gamma_{xs} &= 2\varepsilon_{xs} = \gamma_{xs}^{(0)} + n\kappa_{xs}^{(0)}, \\
\gamma_{xn} &= 2\varepsilon_{xn} = \gamma_{xn}^{(0)},
\end{aligned} \tag{11}$$

where

$$\begin{aligned}
\varepsilon_{xx}^{(0)} &= u_o' + \frac{1}{2}(u_o'^2 + v'^2 + w'^2) + \omega_p\left[\theta' - \frac{1}{2}(\theta_z\theta_y'' - \theta_y\theta_z'')\right] \\
&\quad + \overline{Z}[(-\theta_y' - u_o'\,\theta_y')\cos\phi + (\theta_z' + u_o'\,\theta_z')\,\mathrm{sen}\,\phi] \\
&\quad + \overline{Y}[(-\theta_z' - u_o'\,\theta_z')\cos\phi - (\theta_y' + u_o'\,\theta_y')\,\mathrm{sen}\,\phi] \\
&\quad + \frac{1}{2}\phi'^2(Y^2 + Z^2) + \frac{1}{2}\theta_y'^2\overline{Z}^2 + \frac{1}{2}\theta_z'^2\overline{Y}^2 + \theta_z'\,\theta_y'\,\overline{ZY} \\
&\quad + (z_0\theta_z' - y_0\theta_y')\,\mathrm{sen}\,\phi,
\end{aligned} \tag{12}$$

$$\kappa_{xx}^{(0)} = -\frac{dZ}{ds}[-(\theta_z' + u_0'\,\theta_z')\cos\phi - (\theta_y' + u_0'\,\theta_y')\,\mathrm{sen}\,\phi] + \frac{dY}{ds}[(-\theta_y' - u_0'\,\theta_y')\cos\phi + (\theta_z' + u_0'\,\theta_z')\,\mathrm{sen}\,\phi] - l\left[\theta' - \frac{1}{2}(\theta_z\theta_y'' - \theta_y\theta_z'')\right] - r\phi'^2 - \underline{\overline{Y}\frac{dZ}{ds}\theta_z'^2 + \overline{Z}\frac{dY}{ds}\theta_y'^2 + \left(\overline{Y}\frac{dY}{ds} - \overline{Z}\frac{dZ}{ds}\right)\theta_y'\,\theta_z'}, \tag{13}$$

$$\gamma_{xs}^{(0)} = \frac{dY}{ds}\left[(v' - \theta_z - u_0'\,\theta_z)\cos\phi - z_0\frac{1}{2}(\theta_z\theta_y' - \theta_y\theta_z') + (w' - \theta_y - u_0'\,\theta_y)\sin\phi\right] + (r-\psi)(\phi' - \theta) + \frac{dZ}{ds}\left[(w' - \theta_y - u_0'\,\theta_y)\cos\phi + y_0\frac{1}{2}(\theta_z\theta_y' - \theta_y\theta_z') - (v' - \theta_z - u_0'\,\theta_z)\sin\phi\right] + \psi\left[\phi' - \frac{1}{2}(\theta_z\theta_y' - \theta_y\theta_z')\right], \tag{14}$$

$$\kappa_{xs}^{(0)} = -2[\phi' - \tfrac{1}{2}(\theta_z\theta_y' - \theta_y\theta_z')], \tag{15}$$

$$\gamma_{xn}^{(0)} = \frac{dY}{ds}\left[(w' - \theta_y - u_0'\,\theta_y)\cos\phi + y_0\frac{1}{2}(\theta_z\theta_y' - \theta_y\theta_z') - (v' - \theta_z - u_0'\,\theta_z)\sin\phi\right] - \frac{dZ}{ds}\left[(v' - \theta_z - u_0'\,\theta_z)\cos\phi - z_0\frac{1}{2}(\theta_z\theta_y' - \theta_y\theta_z') + (w' - \theta_y - u_0'\,\theta_y)\sin\phi\right] + l(\phi' - \theta). \tag{16}$$

In comparison with the works carried out by Bhaskar and Librescu [15], Ghorbanpoor and Omidvar [28] and other authors, this model incorporate the deformations corresponding to second-order terms that involve to the axial movement. In this way, appear new components of deformation (terms underlined in the expressions (12) and (13)), which give origin new higher-order effects, as will be indicated later. In the same way, Fraternali and Feo [16] obtained similar strain components, keeping in mind that their formulation corresponds to a non-shear deformable theory.

3.1. Geometric imperfection

To evaluate the structural significance of geometric imperfections, an initial imperfection is defined by some function $v_0(x)$ or $w_0(x)$, corresponding to a lateral and vertical displacement, respectively. These geometric imperfections can be included in the variational formulation by means of a simple concept of initial strains. The strains that result from an initial deflection are as follows:

$$\overline{\varepsilon}_{xx} = \tfrac{1}{2}(v_0'^2 + w_0'^2) - \theta_{y0}'\,\overline{Z} - \theta_{z0}'\,\overline{Y}, \tag{17}$$

$$\overline{\kappa}_{xx} = \theta_{z0}'\,\frac{dZ}{ds} - \theta_{y0}'\,\frac{dY}{ds}, \tag{18}$$

$$\overline{\gamma}_{xs} = (v_0' - \theta_{z0})\frac{dY}{ds} + (w_0' - \theta_{y0})\frac{dZ}{ds}, \tag{19}$$

$$\gamma_{xn}^{(0)} = (w_0' - \theta_{y0})\frac{dY}{ds} - (v_0' - \theta_{z0})\frac{dZ}{ds}. \tag{20}$$

Finally, to consider the imperfections effect on the stability response, the net strains due to the load are defined in the following form:

$$\varepsilon_{xx}^{(1)} = \varepsilon_{xx}^{(0)} - \overline{\varepsilon}_{xx},\ \kappa_{xx}^{(1)} = \kappa_{xx}^{(0)} - \overline{\kappa}_{xx},\ \gamma_{xs}^{(1)} = \gamma_{xs}^{(0)} - \overline{\gamma}_{xs},\ \kappa_{xs}^{(1)} = \kappa_{xs}^{(0)},\ \gamma_{xn}^{(1)} = \gamma_{xn}^{(0)} - \overline{\gamma}_{xn}. \tag{21}$$

4. Variational formulation

Taking into account the adopted assumptions, the principle of virtual work for a composite shell may be expressed in the form:

$$\int\int (N_{xx}\delta\varepsilon_{xx}^{(1)} + M_{xx}\delta\kappa_{xx}^{(1)} + N_{xs}\delta\gamma_{xs}^{(1)} + M_{xs}\delta\kappa_{xs}^{(1)} + N_{xn}\delta\gamma_{xn}^{(1)})\,ds\,dx - \int\int (\overline{q}_x\delta\overline{u}_x + \overline{q}_y\delta\overline{u}_y + \overline{q}_z\delta\overline{u}_z)\,ds\,dx - \int\int (\overline{p}_x\delta u_x + \overline{p}_y\delta u_y + \overline{p}_z\delta u_z)|_{x=0}\,ds\,dn - \int\int (\overline{p}_x\delta u_x + \overline{p}_y\delta u_y + \overline{p}_z\delta u_z)|_{x=L}\,ds\,dn - \int\int\int (\overline{f}_x\delta u_x + \overline{f}_y\delta u_y + \overline{f}_z\delta u_z)\,ds\,dn\,dx = 0, \tag{22}$$

where N_{xx}, N_{xs}, M_{xx}, M_{xs} and N_{xn} are the shell stress resultants [21]. The beam is subjected to wall surface tractions $\overline{q}_x$, $\overline{q}_y$ and $\overline{q}_z$ specified per unit area of the undeformed middle surface and acting along the x, y and z directions, respectively. Similarly, $\overline{p}_x$, $\overline{p}_y$ and $\overline{p}_z$ are the end tractions per unit area of the undeformed cross-section specified at $x=0$ and $x=L$, where L is the undeformed length of the beam. Besides $\overline{f}_x$, $\overline{f}_y$ and $\overline{f}_z$ are the body forces per unit of volume. Finally, denoting $\overline{u}_x$, $\overline{u}_y$ and $\overline{u}_z$ as displacements at the middle line.

5. Constitutive equations and beam forces

The constitutive equations of symmetrically balanced laminates may be expressed in the terms of shell stress resultants in the following form [27]:

$$\begin{Bmatrix} N_{xx} \\ N_{xs} \\ N_{xn} \\ M_{xx} \\ M_{xs} \end{Bmatrix} = \begin{bmatrix} \overline{A}_{11} & 0 & 0 & 0 & 0 \\ 0 & \overline{A}_{66} & 0 & 0 & 0 \\ 0 & 0 & \overline{A}_{55}^{(H)} & 0 & 0 \\ 0 & 0 & 0 & \overline{D}_{11} & 0 \\ 0 & 0 & 0 & 0 & \overline{D}_{66} \end{bmatrix} \begin{Bmatrix} \varepsilon_{xx}^{(1)} \\ \gamma_{xs}^{(1)} \\ \gamma_{xn}^{(1)} \\ \kappa_{xx}^{(1)} \\ \kappa_{xs}^{(1)} \end{Bmatrix}, \tag{23}$$

with

$$\overline{A}_{11} = A_{11} - \frac{A_{12}^2}{A_{22}},\ \overline{A}_{66} = A_{66} - \frac{A_{26}^2}{A_{22}},\ \overline{A}_{55}^{(H)} = A_{55}^{(H)} - \frac{(A_{45}^{(H)})^2}{A_{44}^{(H)}},\ \overline{D}_{11} = D_{11} - \frac{D_{12}^2}{D_{22}},\ \overline{D}_{66} = D_{66} - \frac{D_{26}^2}{D_{22}}, \tag{24}$$

where A_{ij}, D_{ij} and $A_{ij}^{(H)}$ are plate stiffness coefficients defined according to the lamination theory presented by Barbero [27]. The coefficient $\overline{D}_{16}$ has been neglected because of its low value for the considered laminate stacking sequence [29].

Substituting expressions (21) into (22) and integrating with respect to s, one obtains the one-dimensional expression for the virtual work equation [21]. The beam forces, in terms of the shell stress resultants, are defined in this last equation by the following form:

$$N = \int N_{xx}ds,\ M_Y = \int\left(N_{xx}\overline{Z} + M_{xx}\frac{dY}{ds}\right)ds,\ M_Z = \int\left(N_{xx}\overline{Y} - M_{xx}\frac{dZ}{ds}\right)ds,$$

$$Q_Z = \int\left(N_{xs}\frac{dZ}{ds} + N_{xn}\frac{dY}{ds}\right)ds,\ Q_Y = \int\left(N_{xs}\frac{dY}{ds} - N_{xn}\frac{dZ}{ds}\right)ds,\ T_w = \int (N_{xs}(r-\psi) + N_{xn}l)ds,$$

$$B = \int (N_{xx}\omega_p - M_{xx}l)ds,\ T_{sv} = \int (N_{xs}\psi - 2M_{xs})ds, \tag{25}$$

where, N corresponds to the axial force, Q_y and Q_z to shear forces, M_y and M_z to bending moments about $\overline{y}$ and $\overline{z}$ axis, respectively, B to the bimoment, T_w to the flexural–torsional moment and T_{sv} to the Saint-Venant torsional moment. Furthermore, ω_p is the

contour warping function, $r(s)$ represents the perpendicular distance from the shear center (SC) to the tangent at any point of the mid-surface contour, and $l(s)$ represents the perpendicular distance from the shear center (SC) to the normal at any point of the mid-surface contour. Finally, Ψ is the shear strain at the middle line [14]. In addition, four high-order stress resultants have been defined.

$$B_1 = \int [N_{xx}(Y^2+Z^2) - 2M_{xx}r]ds, P_{yy} = \int \left[N_{xx}\overline{Z}^2 + 2M_{xx}\overline{Z}\frac{dY}{ds}\right]ds,$$

$$P_{zz} = \int \left[N_{xx}\overline{Y}^2 - 2M_{xx}\overline{Y}\frac{dZ}{ds}\right]ds, P_{yz} = \int \left[N_{xx}\overline{YZ} + M_{xx}\left(\overline{Y}\frac{dY}{ds} - \overline{Z}\frac{dZ}{ds}\right)\right]ds. \tag{26}$$

In expressions (25) and (26) the integration is carried out over the entire length of the mid-line contour.

The relations among the generalized beam forces and the generalized strains characterizing the behavior of the beam are obtained by substituting the expressions (21) into (23), and then the results into the shell stress resultants (25–26). In this way, the constitutive law can be expressed in terms of a beam stiffness matrix as defined in [21]. On the other hand, the generalized strains can be identified in terms of the beam forces and moments, as:

$$\begin{aligned}
&\textit{corresponding to } N: \quad ED_1 = u_0' + \tfrac{1}{2}(u_0'^2 + v'^2 + w'^2 + v_0'^2 + w_0'^2) \\
&\qquad + (z_0\theta_z' - y_0\theta_y')sen\phi, \\
&\textit{corresponding to } M_y: \quad ED_2 = (-\theta_y' - u_0'\,\theta_y')\cos\phi + \theta_{y0}' \\
&\qquad + (\theta_z' + u_0'\,\theta_z')sen\,\phi, \\
&\textit{corresponding to } M_z: \quad ED_3 = (-\theta_z' - u_0'\,\theta_z')\cos\phi + \theta_{z0}' \\
&\qquad - (\theta_y' + u_0'\,\theta_y')sen\,\phi, \\
&\textit{corresponding to } B: \quad ED_4 = \theta' - \tfrac{1}{2}(\theta_z\theta_y'' - \theta_y\theta_z''), \\
&\textit{corresponding to } Q_y: \quad ED_5 = (v' - \theta_z - u_0'\,\theta_z)\cos\phi - v_0' + \theta_{z0} \\
&\qquad - z_0\tfrac{1}{2}(\theta_z\theta_y' - \theta_y\theta_z') + (w' - \theta_y - u_0'\,\theta_y)sen\,\phi, \\
&\textit{corresponding to } Q_z: \quad ED_6 = (w' - \theta_y - u_0'\,\theta_y)\cos\phi \\
&\qquad - w_0' + \theta_{y0} + y_0\tfrac{1}{2}(\theta_z\theta_y' - \theta_y\theta_z') \\
&\qquad - (v' - \theta_z - u_0'\,\theta_z)sen\,\phi, \\
&\textit{corresponding to } T_w: \quad ED_7 = \phi' - \theta, \\
&\textit{corresponding to } T_{sv}: \quad ED_8 = \phi' - \tfrac{1}{2}(\theta_z\theta_y' - \theta_y\theta_z'), \\
&\textit{corresponding to } B_1: \quad ED_9 = \frac{\phi'^2}{2}, \\
&\textit{corresponding to } P_{yy}: \quad ED_{10} = \frac{\theta_y'^2}{2}, \\
&\textit{corresponding to } P_{zz}: \quad ED_{11} = \frac{\theta_z'^2}{2}, \\
&\textit{corresponding to } P_{yz}: \quad ED_{12} = \theta_y'\,\theta_z'.
\end{aligned} \tag{27}$$

These generalized strains correspond to the axial strain (ED_1), the two bending curvatures (ED_2 and ED_3), the torsional curvature (ED_4), the two transverse shear strain (ED_5 and ED_6), the transverse shear strain due to warping (ED_7), the rate of twist and a non-linear term (ED_8 and ED_9), the higher-order axial terms (ED_{10}, ED_{11} and ED_{12}).

6. The discrete equilibrium problem

In order to perform the non-linear analysis the Ritz variational method is used for reducing the governing equation in terms of generalized coordinates. From the reduced system, first the buckling loads are determined from the singularity condition of the tangent stiffness matrix determinant of the structure [14,18]. Then, an incremental-iterative method based on the Newton–Raphson method combined with constant arc length is employed for the solution of non-linear equilibrium equation. The equations of motion are discretized to analyze the stability behavior of simply supported and fixed-end beams.In the case of simply supported beams, the displacements modes are approximated by means of the following functions, which are compatible with the boundary conditions of the beam:

$$\begin{aligned}
&u_0 = U\frac{x}{L}, \\
&v = V\sin\left(\frac{\pi}{L}x\right), \theta_z = \Theta_z\cos\left(\frac{\pi}{L}x\right), \\
&w = W\sin\left(\frac{\pi}{L}x\right), \theta_y = \Theta_y\cos\left(\frac{\pi}{L}x\right), \\
&\phi = \Phi\sin\left(\frac{\pi}{L}x\right), \theta = \Theta\cos\left(\frac{\pi}{L}x\right),
\end{aligned} \tag{28}$$

where U, V, W, Θ_z, Θ_y, Φ and Θ are the associated displacement amplitudes. Besides, the initial deflection can be expressed as:

$$w_0 = W_0\sin\left(\frac{\pi}{L}x\right), \theta_{y0} = \varphi_{y0}\cos\left(\frac{\pi}{L}x\right), \tag{29}$$

$$v_0 = V_0\sin\left(\frac{\pi}{L}x\right), \theta_{z0} = \varphi_{z0}\cos\left(\frac{\pi}{L}x\right). \tag{30}$$

For the case of fixed-end beams, the variational equation is discretized by using beam characteristic orthogonal polynomials which satisfy the geometrical boundary conditions and are generated by using the Gram-Schmidt process.

$$U = \sum_{i=1}^{n} c_i\xi_i(x) \tag{31}$$

where U represent each of the displacements and c_i are the undetermined arbitrary coefficients. The polynomials $\xi_i(x)$ are generated as follows [30]:

$$\xi_2(x) = (x - B_2)\xi_1(x), \ldots, \xi_k(x) = (x - B_k)\xi_{k-1}(x) - C_k\xi_{k-2}(x),$$

Where

$$B_k = \frac{\int_0^L x\xi_{k-1}^2(x)dx}{\int_0^L \xi_{k-1}^2(x)dx}, C_k = \frac{\int_0^L x\xi_{k-1}(x)\xi_{k-2}(x)dx}{\int_0^L \xi_{k-2}^2 dx}. \tag{32}$$

The first member of the orthogonal polynomial $\xi_1(x)$ is chosen as the simplest polynomial (of the least order) that satisfies the boundary conditions. In order to obtain sufficient accurate results, four terms (n=4) are taken for each one of the flexural–torsional displacements. As in the previous case, the initial deflection can be expressed as:

$$w_0 = W_0\frac{1}{2}\left[1 - \cos\left(\frac{2\pi}{L}x\right)\right], \theta_{y0} = \varphi_{y0}\sin\left(\frac{2\pi}{L}x\right), \tag{33}$$

$$v_0 = V_0\frac{1}{2}\left[1 - \cos\left(\frac{2\pi}{L}x\right)\right], \theta_{z0} = \varphi_{z0}\sin\left(\frac{2\pi}{L}x\right). \tag{34}$$

After integration along the beam length according to the adopted functions for the displacements, a coupled and strongly non-linear algebraic system is obtained. This resulting system has an extremely complicated form, for this reason, it is not presented here.

7. Applications and numerical results

The purpose of this section is to apply the simple present approach for determining the influence of imperfection on the buckling, prebuckling and postbuckling behavior of thin-walled composite beams. The fundamental and secondary equilibrium paths of perfect and imperfect systems are analyzed for the case of flexural and flexural–torsional stability behavior of a thin-walled composite beam. The numerical results are obtained for a four layer bisymmetric-I cross-section (Fig. 3), whose geometrical properties are h=0.6 m, b=0.6 m and e=0.03 m. The analyzed material is glass/epoxy whose properties are E_1=48.3 GPa, E_2=19.8 GPa, G_{12}=8.96 GPa, G_{13}=8.96 GPa, G_{23}=6.19 GPa, ν_{12}=0.27, ν_{13}=0.27, ν_{23}=0.6, ρ=1389 kg/m^3.

7.1. Buckling of simply supported beam subjected to an axial force

The first example corresponds to a simply supported beam subjected to an axial load applied to the centroid. The non-linear equilibrium equations are uncoupled in this case, there are three buckling modes corresponding either to bending or torsion (see Fig. 4). The influence of imperfections is analyzed on the torsional buckling mode. In the case of a perfect beam, the critical load corresponding to the torsional mode can be easily obtained by means of Eq. (35) (as explained by the author in Ref. [14]):

$$P_\phi = \frac{L^2\widehat{GS}_w\widehat{GJ} + \widehat{EC}_w\pi^2(\widehat{GJ}+\widehat{GS}_w)}{I_0(\widehat{GS}_wL^2+\widehat{EC}_w\pi^2)}, \tag{35}$$

where, $\widehat{EC}_w$, $\widehat{GJ}$ and $\widehat{GS}_w$ are the warping, torsional and shear stiffness of a composite beam (for isotropic beams the same expressions are applicable without the "hats" [14]). I_0 is the polar moment of inertia about shear center.

On the other hand, to consider the imperfection effect on the buckling response, it is assume that the critical load of torsional buckling is smaller than flexural critical load about z-axis. Therefore, it is possible to find the solution of the displacement field in the vertical motion $\{u, v, \theta_z, w, \theta_y, \phi, \theta\}^t$=$\{0, 0, 0, w, \theta_y, 0, 0\}^t$, for a given shape of initial deflection w_0. This vertical displacement is obtained from the linearized version of Eq. (22). In fact, by neglecting all the non-linear terms in Exp. (22), and applying the variational calculus, the differential equations of equilibrium are obtained which are easily solved in a closed form in order to determine the displacements in the vertical plane. For the case of simply supported beams subjected to an axial load, the amplitudes corresponding to the vertical displacements are given

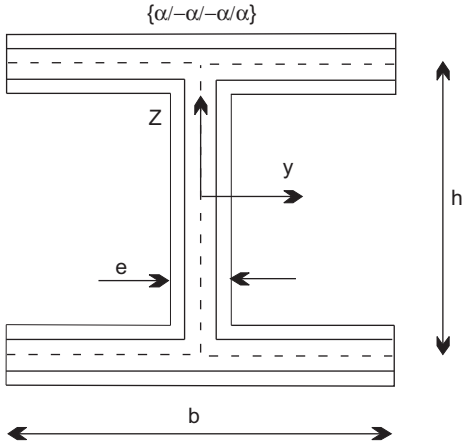

Fig. 3. Analyzed cross-section shape.

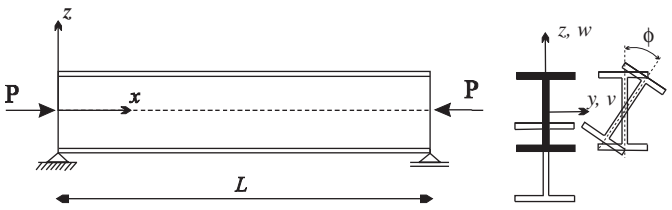

Fig. 4. Simply supported beam subjected to axial load and buckling shapes modes.

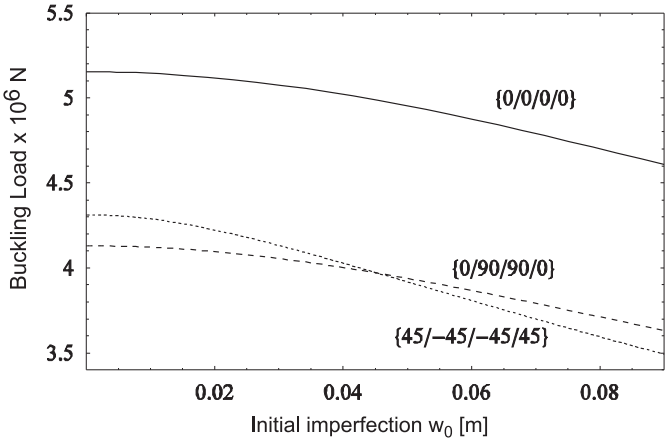

Fig. 5. Influence of initial vertical imperfection w_0 on the buckling load, L=12 m.

by the following expressions:

$$W = \frac{w_0}{1+\dfrac{P}{P_y}}, \Theta_y = \frac{P_y}{\widehat{EI}_y}\frac{L}{\pi}W, \tag{36}$$

where P_y is the flexural critical load of a perfect beam [14]:

$$P_y = \frac{\widehat{EI}_y\widehat{GS}_z\pi^2}{\widehat{GS}_zL^2+\widehat{EI}_y\pi^2}, \tag{37}$$

where $\widehat{EI}_y$ is the flexural stiffness and $\widehat{GS}_z$ is the shear stiffness of a composite beam. To determine the torsional buckling considering an initial imperfection w_0, Exp. (36) is substituted into (22), the lateral displacements v and θ_z are neglected and the remaining displacements ϕ and θ are discretized in the resultant variational equation by means of the trigonometric functions defined in (28). This procedure leads to the algebraic expression for the unknown P. The solution of this equation permits to determine the critical load of torsional buckling.

Figs. 5 and 6 show the effect of an initial vertical deflection (z-axis) on the buckling load, considering two beam lengths and three stacking sequences of lamination.

It is possible to appreciate in the figures that the effect of imperfections is to reduce the buckling load values with respect to the perfect beam. The difference between perfect and imperfect system becomes more significant as increase the vertical initial imperfection. This effect depends on the stacking sequence and the beam length. In this example, the lamination $\{45/-45/-45/45\}$ presents higher influence to the imperfection effect than the other sequences. In addition, this effect is larger when the beam slenderness increases. For example, when the beam length is L=12 m, the perceptual difference between the perfect and imperfect buckling loads is about 20%, considering an initial imperfection w_0=0.09 m. However, the difference is about 10% when the fibers are oriented in the longitudinal direction. Therefore, it is found that the influence of the imperfection effect decreases as the beam stiffness increases.

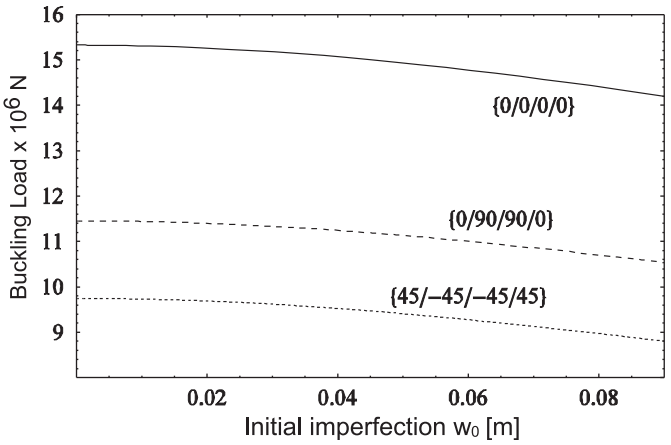

Fig. 6. Influence of initial vertical imperfection w_0 on the buckling load, L=6 m.

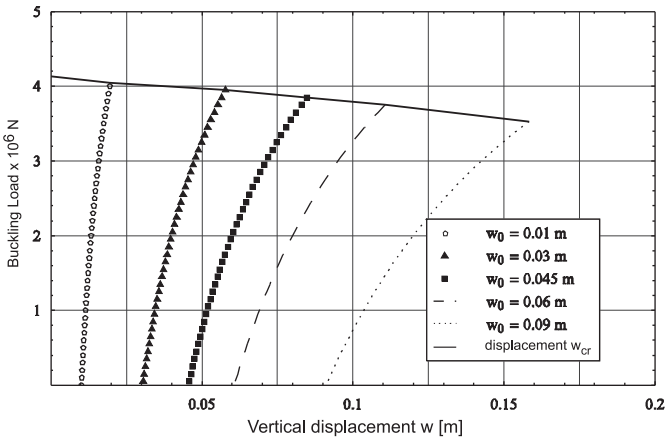

Fig. 8. Imperfection effect on the fundamental path, lamination {0/90/90/0}.

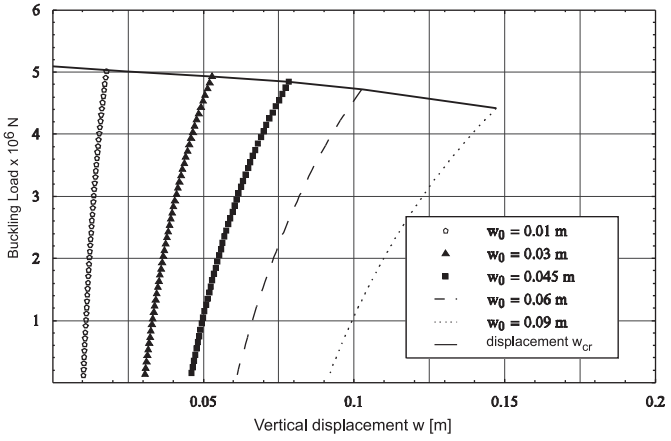

Fig. 7. Imperfection effect on the fundamental path, lamination {0/0/0/0}.

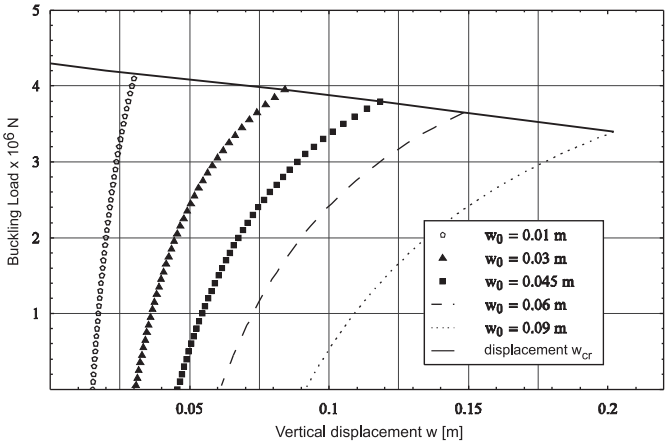

Fig. 9. Imperfection effect on the fundamental path, lamination {45/−45/−45/45}.

7.2. *Prebuckling and postbuckling of simply supported beam subjected to an axial force*

The effect of imperfections is analyzed on the prebuckling and postbuckling behavior of a simply supported beam subjected to an axial load, for a beam length L=12 m. The fundamental path of the vertical displacement for different initial deflection values is shown in Figs. 7–9, for a sequence of lamination {0/0/0/0}, {0/90/90/0} and {45/−45/−45/45}, respectively.

It can be observed from the figures that the reduction of the buckling load values is associated with an increase in the vertical displacement to the bifurcation load. As in the buckling state, the displacement values of the lamination {45/−45/−45/45} are larger in comparison with the other laminations; it is due mainly to the flexibility effect. Therefore, the imperfection effect on the fundamental state is also more significant for this lamination. This effect is clearly verified following the solid line which connects the maximum displacements for each imperfection value. For example, considering an initial imperfection of w_0=0.09 m, the critical displacement is w_{cr}=0.147 m for a lamination {0/0/0/0}, while for the lamination {45/−45/−45/45} is w_{cr}=0.2 m. This behavior was also observed in the previous section, where the imperfection influence on the buckling behavior depended on the beam stiffness. The lamination sequence {0/90/90/0} presents an intermediate flexibility between {45/−45/−45/45} and {0/0/0/0}.

The equilibrium paths of perfect and imperfect systems are investigated for the non-linear torsional stability behavior. It is shown in the Figs. 10–12, the influence of the major imperfections on the postbuckling response, for a sequence of lamination {0/0/0/0}, {0/90/90/0} and {45/−45/−45/45}, respectively. The load-twisting curves are stable and symmetric for all the cases analyzed. The beam stability is not influenced by the imperfection effect. In the case of perfect beams, the bifurcation loads correspond to the buckling load calculated in the first example 7.1. However, as the imperfection values increase, it is not

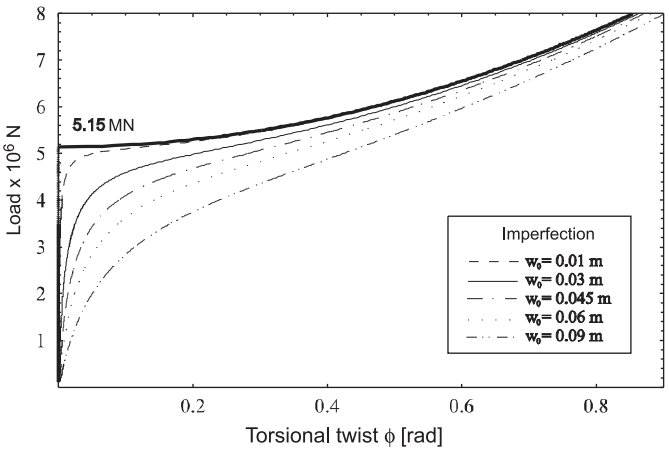

Fig. 10. Influence of imperfections on the postbuckling behavior, lamination {0/0/0/0}.

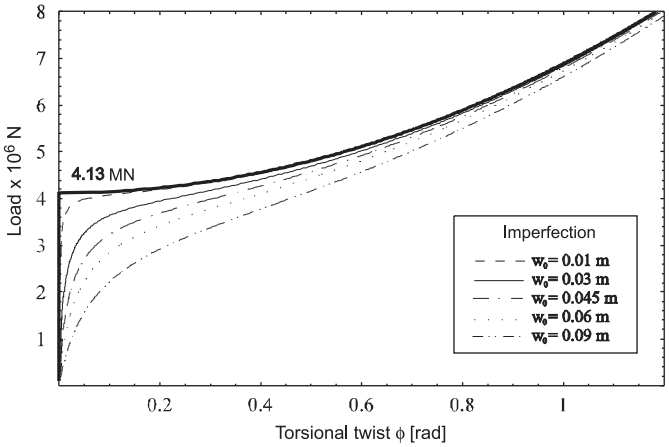

Fig. 11. Influence of imperfections on the postbuckling behavior, lamination {0/90/90/0}.

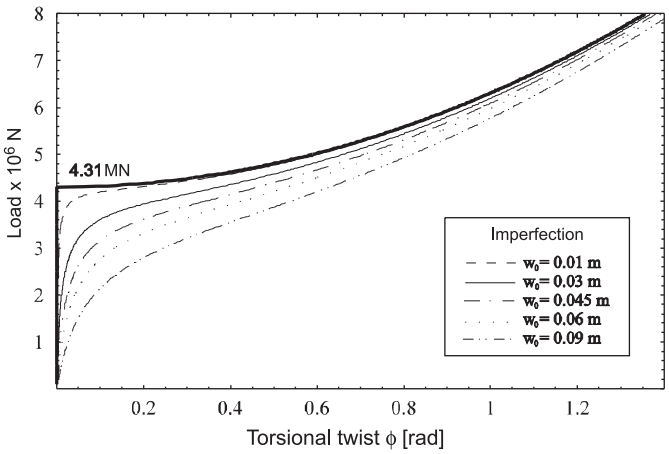

Fig. 12. Influence of imperfections on the postbuckling behavior, lamination {45/−45/−45/45}.

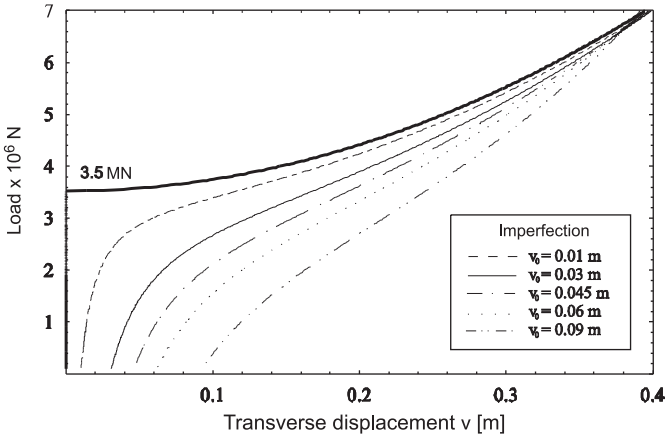

Fig. 13. Postcritical path considering transverse imperfection, lamination {0/0/0/0}.

so clear to determine the bifurcation load. It can be observed from the figures that the critical point disappears due to a major imperfection for the torsional twist postbuckling response. On the other hand, the unidirectional lamination {0/0/0/0} has the highest buckling load and the larger additional load carrying capacity after buckling. The lamination {0/90/90/0} has the lowest critical load and the lamination {45/−45/−45/45} presents the

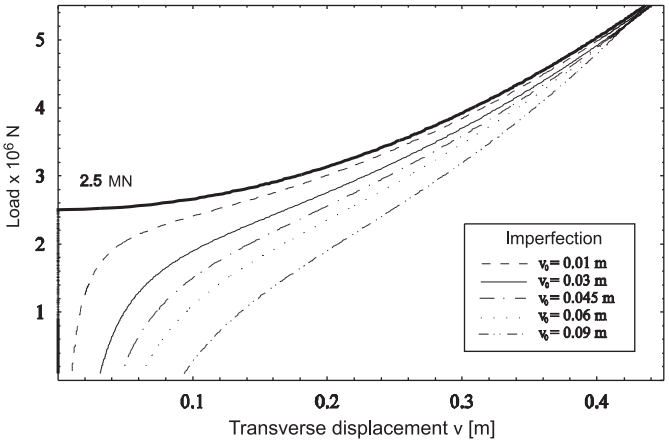

Fig. 14. Postcritical path considering transverse imperfection, lamination {0/90/90/0}.

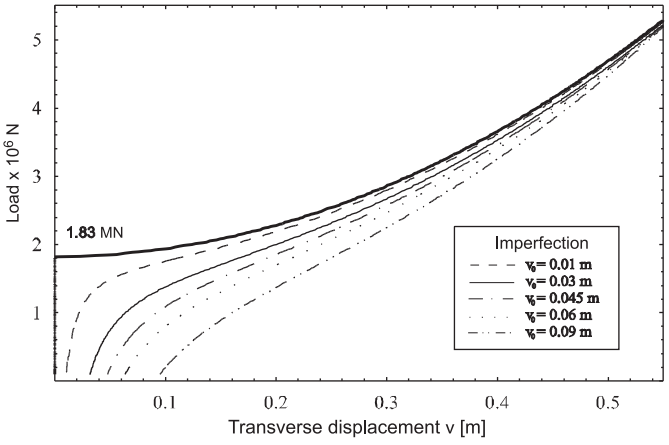

Fig. 15. Postcritical path considering transverse imperfection, lamination {45/−45/−45/45}.

smaller additional load capacity. The imperfection effect reduces the values of the equilibrium path with respect to the perfect condition. However, the margins of postbuckling strength are not influenced by the imperfection effect. This behavior is mainly due to the structural flexibility, allowing moderate large displacements in the imperfect postbuckling curves which converge into the perfect curves as the displacement increases.

7.3. Postbuckling of simply supported beam with transverse imperfection

As in the previous example the same boundary condition is considered, but in this case the effect of transverse imperfections (see Exp. (30)) on postbuckling behavior is analyzed. The effect of imperfections on the fundamental path corresponding to the lateral displacement (y-axis) is shown in Figs. 13–15, for a sequence of lamination {0/0/0/0}, {0/90/90/0} and {45/−45/−45/45}, respectively. For a bisymmetric simply supported beam subjected to an axial load, the smallest buckling mode corresponds to a bending mode in the y-direction, while the second buckling mode corresponds to the torsional twist. Therefore, the bifurcation points are smaller than in the previous example. The load-deflection curves are symmetric and stable in all the cases analyzed. The stacking sequence {0/0/0/0} presents the highest buckling load and the largest load carrying capacity after buckling. The imperfections effect is higher for the lamination {45/−45/−45/45}, where the imperfect postbuckling

curves converge into the perfect curves for larger displacement values.

7.4. Lateral postbuckling of a fixed-end beam

A fixed-end beam loaded by a transverse force at the middle of the span is considered. The vertical force is applied on the top flange for a beam length $L=12$ m. When the beam is loaded in its plane of symmetry it initially deflects. However, at a certain level of the applied load, the beam may buckle laterally, while the cross-sections of the beam rotate simultaneously about the beam's axis. This phenomenon is called lateral buckling, and the load value at which buckling occurs is the critical load. As in the previous example, an initial transverse imperfection in the y-direction is considered (see, Exp. (34)) to study the flexural–torsional postbuckling behavior. The imperfect postbuckling paths, corresponding to the torsional amplitude ϕ, are shown in Figs. 16–18. Three different magnitudes of imperfection are analyzed for the stacking sequences {0/0/0/0}, {0/90/90/0} and {45/−45/−45/45}. Furthermore, the accuracy of the proposed formulation is checked by comparing results with those solutions obtained by Abaqus's shell element. The beam is idealized by 240 four-node shell elements (S4). The finite element analysis is based on two steps. First, a static linear analysis is performed on the "perfect" structure to use the response as an imperfection state. In the second analysis an imperfection is introduced in the geometry by addition of the static displacement to the "perfect" geometry using the IMPERFECTION option. A geometrically non-linear load-displacement analysis of the structure containing the imperfections is performed using the Riks method. In this way, the Riks method can be used to perform postbuckling analyzes.

In this case, the shape of the imperfection corresponds to the flexural mode of a fixed-end beam subjected to a distributed load applied in the y-direction (see Fig. 19). The imperfection magnitudes are included in the model as a scale factor of the flexural mode amplitude.

The postbuckling equilibrium paths are stable and symmetric for all the cases studied. The deformed state of the thin-walled beam obtained with Abaqus is shown in Fig. 20, considering an imperfection $v_0=0.045$ m and a lamination {0/90/90/0}. It can be seen that the postbuckling deformed shape correspond to a flexural–torsional mode. It is important to note that a local buckling mode appears in the top flange of the beam (see Fig. 20). The presence of this effect can be due to the concentrated force, which is precisely applied in this place. However, the influence of this local mode on the global postbuckling response is not enough to modify considerably the beam stability behavior. On the other hand, the postbuckling curves are drawn with the twist values measured from the centroid of the cross-section. Finally, the postbuckling behavior obtained with the shell model is, in general, in good agreement with those obtained with the present beam model.

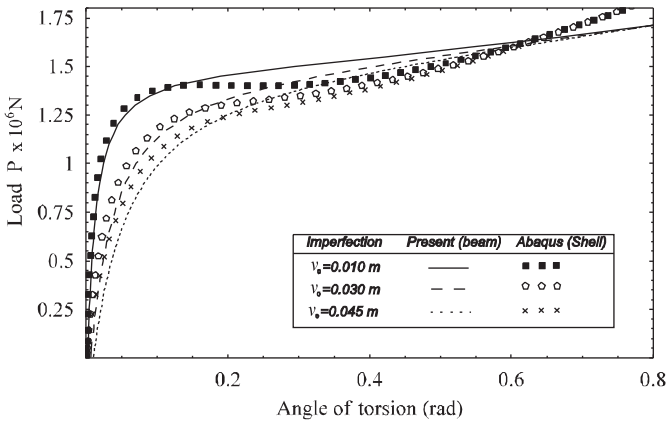

Fig. 16. Lateral postbuckling behavior considering the influence of imperfection, lamination {0/0/0/0}.

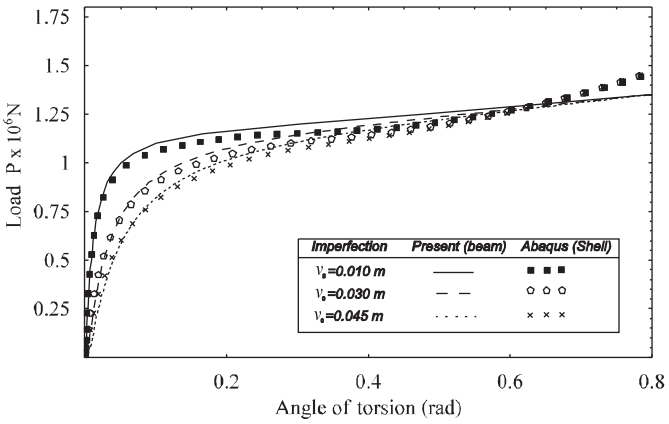

Fig. 17. Lateral postbuckling behavior considering the influence of imperfection, lamination {0/90/90/0}.

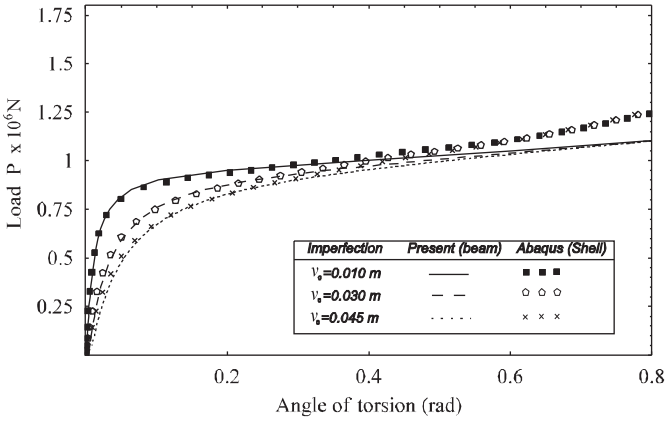

Fig. 18. Lateral postbuckling behavior considering the influence of imperfection, lamination {45/−45/−45/45}.

8. Conclusions

This paper presents a theory to account for changes in the stability behavior of thin-walled composite beams when design parameters are modified. In particular, the model takes into account the influence of geometrical imperfections on the buckling, prebuckling and postbuckling beam response. A geometrically non-linear beam theory is used to investigate the influence of imperfections for simply supported and fixed-end beams subjected to axial and lateral loads. Therefore, the flexural, torsional and flexural–torsional stability is analyzed by means of a beam model formulated in the context of large displacements and rotations. The theory is based on a shear deformable displacement field (accounting for bending and warping shear), considering moderate bending rotations and large torsional twist. The Ritz's method is used to obtain an algebraic system, which is solved by an incremental Newton–Raphson algorithm. A set of beam characteristic orthogonal polynomials and trigonometric functions are used to discretize the variational equation.

Numerical results corresponding to the fundamental and equilibrium paths of perfect and imperfect systems have been presented, considering major imperfections of various

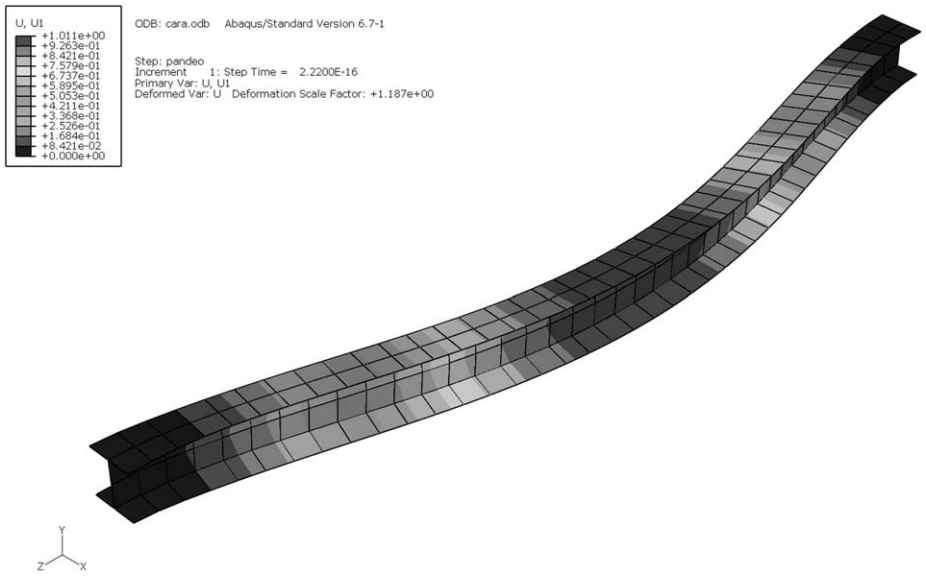

Fig. 19. Deformed shape, corresponding to the first static step, used as a geometric imperfection.

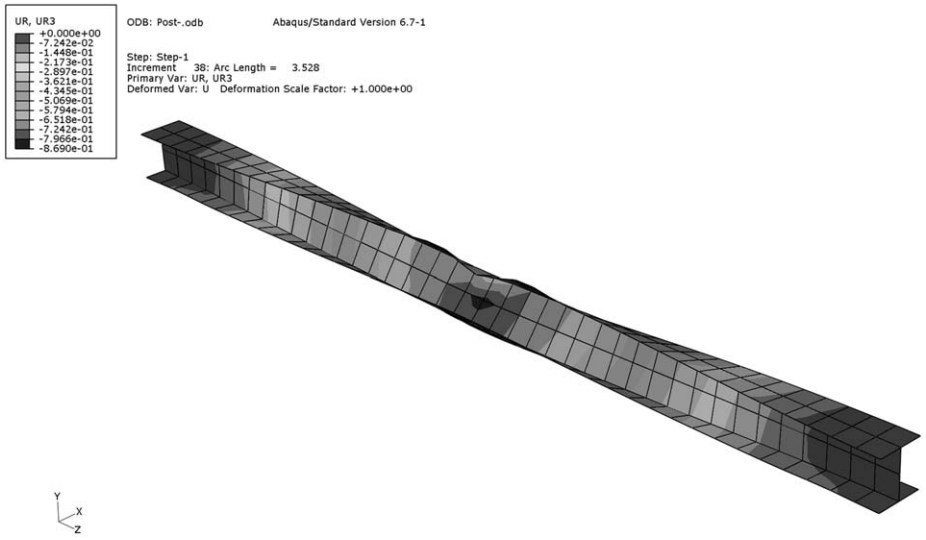

Fig. 20. Lateral postbuckling state of a fixed-end imperfect beam, v_0=0.045 m.

magnitudes. It has been shown that in presence of imperfections the stability of a flexible structure, allowing moderately large displacements, is not modified with respect to the perfect case. The postbuckling curves were stable and symmetric in all the cases analyzed. However, the critical buckling load is reduced by the effect of geometrical imperfections. This effect depends on the stacking sequences and the beam length used. It was found that the lamination $\{45/-45/-45/45\}$ presents a higher imperfection influence on the buckling response than the other sequences of behavior was observed lamination considered. A similar in the prebuckling state, where the lamination $\{45/-45/-45/45\}$ presented the larger displacement values to the critical condition. It was determined that the reduction of the buckling load values is associated with an increase in the vertical displacement to the bifurcation load. Therefore, it was concluded that the imperfection effect depends on the stiffness of the structure and the influence of this effect decreases as the beam stiffness increases.

It was found that the beam formulation proposed in this paper predicts correctly the 3-D non-linear elastic response of thin-walled composite beams. The postbuckling behavior obtained with the present model is, in general, in good agreement with those obtained with a shell finite element model using Abaqus. It is a very important issue because the computational cost demanded by the 3-D shell model was substantially larger than those used by the present beam model.

As a conclusion, the buckling and postbuckling behavior of thin-walled composite beams is influenced by the imperfection effect. The effect of initial transverse imperfection reduces the buckling loads and makes the postbuckling equilibrium paths be lower in comparison with the perfect one. Furthermore, these effects become larger as the initial deflections increases.

Acknowledgments

The present study was sponsored by Secretaría de Ciencia y Tecnología, Universidad Tecnológica Nacional, and by CONICET.

References

[1] V.Z. Vlasov, Thin-walled elastic beams, Jerusalem: Israel Program for Scientific Translation; 1961.
[2] J.F. Davalos, P. Qiao, Analytical and experimental study of lateral and distorsional buckling of FRP wide-flange beams, ASCE J. Compos. Constr. 1 (4) (1997) 150–159.
[3] R.S. Barsoum, R.H. Gallagher, Finite element analysis of torsional and torsional-flexural stability problems, Int. J. Numer. Methods Eng. 2 (1970) 335–352.
[4] S.T. Woolcock, A.M. Trahair, Post-buckling behavior of determinate beams, J. Eng. Mech. Div. ASCE 100 (1974) 151–171.
[5] H. Chen, G.E. Blandford, Thin-walled space frames. II: algorithmic details and applications, J. Struct. Eng. ASCE 117 (1991) 2521–2539.
[6] K.M. Hsiao, W.Y. Lin, A co-rotational finite element formulation for buckling and postbuckling analysis of spatial beams, Comput. Methods Appl. Mech. Eng. 188 (2000) 567–594.
[7] K.M. Hsiao, W.Y. Lin, A co-rotational formulation for thin-walled beams with monosymmetric open section, Comput. Methods Appl. Mech. Eng. 190 (2000) 1163–1185.
[8] W.Y. Lin, K.M. Hsiao, Co-rotational formulation for geometric non-linear analysis of doubly-symmetric thin-walled beams, Comput. Methods Appl. Mech. Eng. 190 (2001) 6023–6052.
[9] F. Mohri, L. Azrar, M. Potier-Ferry, Lateral post-buckling analysis of thin-walled open sections beams, Thin-walled Struct. 40 (2002) 1013–1036.
[10] Y.L. Pi, M.A. Bradford, Effects of approximations in analysis of beams of open thin-walled cross-section—part II: 3-D non-linear behaviour, Int. J. Numer. Methods Eng. 51 (2001) 773–790.
[11] Y.L. Pi, M.A. Bradford, Elastic flexural–torsional buckling of continuously restrained arches, Int. J. Solids Struct. 39 (2002) 2299–2322.
[12] Y.L. Pi, M.A. Bradford, Effects of prebuckling deformations on the elastic flexural–torsional buckling of laterally fixed arches, Int. J. Mech. Sci. 46 (2004) 321–342.
[13] Y.L. Pi, M.A. Bradford, F. Tin-Loi, Flexural–torsional buckling of shallow arches with open thin-walled section under uniform radial loads, Thin-walled Struct. 45 (2007) 352–362.
[14] S.P. Machado, Non-linear buckling and postbuckling behavior of thin-walled beams considering shear deformation, Int. J. Non-linear Mech. 43 (2008) 345–365.
[15] K. Bhaskar, L. Librescu, A geometrically non-linear theory for laminated anisotropic thin-walled beams, Int. J. Eng. Sci. 33 (1995) 1331–1344.
[16] F. Fraternali, L. Feo, On a moderate rotation theory of thin-walled composite beams, Compos. Part B Eng. 31 (2002) 141–158.
[17] A. Sapkás, L.P. Kollár, Lateral-torsional buckling of composite beams, Int. J. Solids Struct. 39 (2002) 2939–2963.
[18] S.P. Machado, V.H. Cortínez, Lateral buckling of thin-walled composite bisymmetric beams with prebuckling and shear deformation, Eng. Struct. 27 (2005) 1185–1196.
[19] T.A. Morey, E. Johnson, C.K. Shield, A simple beam theory for the buckling on symmetric composite beams including interaction of in-plane stresses, Compos. Sci. Tech. 58 (1998) 1321–1333.
[20] S.Y. Back, K.M. Will, Shear-flexible thin-walled element for composite I-beams, Eng. Struct. 30 (2008) 1447–1458.
[21] S.P. Machado, V.H. Cortínez, Non-linear model for stability of thin-walled composite beams with shear deformation, Thin-walled Struct. 43 (2005) 1615–1645.
[22] J.M. Thompson, G.W. Hunt, A General Theory of Elastic Stability, Wiley, London, 1973.
[23] F. Flores, L.A. Godoy, Elastic post-buckling analysis via finite element and perturbation techniques, part I: formulation, Int. J. Numer. Methods Eng. 33 (1992) 1775–1794.
[24] L.A. Godoy, Thin-walled Structures with Imperfections: Analysis and Behavior, Elsevier, London, 1996.
[25] C. Szymczak, Sensitivity analysis of thin-walled members, problems and applications, Thin-walled Struct. 41 (2003) 271–290.
[26] J. Chróscielewski, I. Lubowiecka, C. Szymczak, W. Witkowski, On some aspects of torsional buckling of thin-walled I-beam columns, Comput. Struct. 84 (2006) 1946–1957.
[27] E.J. Barbero, Introduction to Composite Material Design, Taylor and Francis Inc, 1999.
[28] A. Ghorbanpoor, B. Omidvar, Non linear FE solution for thin-walled open section composite members, J. Struct. Eng. ASCE 122 (1996) 1369–1378.
[29] V.H. Cortínez, M.T. Piovan, Vibration and buckling of composite thin-walled beams with shear deformability, J. Sound Vib. 258 (2002) 701–723.
[30] R.B. Bhat, Transverse vibrations of a rotating uniform cantilever beam with tip mass as predicted by using beam characteristic orthogonal polynomials in the Rayleigh–Ritz method, J. Sound Vib. 105 (1986) 199–210.